



**HAL**  
open science

**The necessity of investigating a freshwater-marine continuum using a mesocosm approach in nanosafety: The case study of TiO<sub>2</sub> MNM-based photocatalytic cement**

Amélie Châtel, Melanie Auffan, Hanane Perrein-Ettajani, Lenka Brousset, Isabelle Métails, Perrine Chaurand, Mohammed Mouloud, Simon Clavaguera, Yohann Gandolfo, Mélanie Bruneau, et al.

► **To cite this version:**

Amélie Châtel, Melanie Auffan, Hanane Perrein-Ettajani, Lenka Brousset, Isabelle Métails, et al.. The necessity of investigating a freshwater-marine continuum using a mesocosm approach in nanosafety: The case study of TiO<sub>2</sub> MNM-based photocatalytic cement. *NanoImpact*, 2020, 20, pp.1-8. 10.1016/j.impact.2020.100254. hal-02971510

**HAL Id: hal-02971510**

**<https://hal.science/hal-02971510>**

Submitted on 21 Dec 2020

**HAL** is a multi-disciplinary open access archive for the deposit and dissemination of scientific research documents, whether they are published or not. The documents may come from teaching and research institutions in France or abroad, or from public or private research centers.

L'archive ouverte pluridisciplinaire **HAL**, est destinée au dépôt et à la diffusion de documents scientifiques de niveau recherche, publiés ou non, émanant des établissements d'enseignement et de recherche français ou étrangers, des laboratoires publics ou privés.

1 ***The necessity of investigating a freshwater-marine continuum using a mesocosm approach***  
2 ***in nanosafety: the case study of TiO<sub>2</sub> MNM-based photocatalytic cement***

3 Amélie Châtel<sup>1\*</sup>, Mélanie Auffan<sup>2,3</sup>, Hanane Perrein-Ettajani<sup>1</sup>, Lenka Brousset<sup>4</sup>, Isabelle  
4 Métails<sup>1</sup>, Perrine Chaurand<sup>2</sup>, Mohammed Mouloud<sup>1</sup>, Simon Clavaguera<sup>5</sup>, Yohann Gandolfo<sup>1</sup>,  
5 Mélanie Bruneau<sup>1</sup>, Armand Masion<sup>2</sup>, Alain Thiéry<sup>4</sup>, Jérôme Rose<sup>2,3</sup>, Catherine Mouneyrac<sup>1</sup>

6 <sup>1</sup>Laboratoire Mer, Molécules, Santé (MMS, EA 2160); Université Catholique de l'Ouest, Angers F-49000 France

7 <sup>2</sup>CEREGE, CNRS, Aix Marseille Univ, IRD, INRA, Coll France, Aix-en-Provence, France

8 <sup>3</sup>Duke University, Civil and Environmental Engineering, Durham, USA

9 <sup>4</sup>Aix Marseille Université, Avignon Université, CNRS, IRD, IMBE UMR 7263, FR— 13284, Marseille

10 <sup>5</sup>Université Grenoble Alpes, Commissariat à l'Energie Atomique et aux Energies Alternatives (CEA), LITEN, NanoSafety  
11 Platform, F-38054 Grenoble, France

12 [\\*amelie.chatel@uco.fr](mailto:*amelie.chatel@uco.fr)

13 **Abstract**

14 Production of Manufactured Nanomaterials (MNMs) has increased extensively due to  
15 economic interest in the current years. However, this widespread use raises concern about  
16 their impact on human and environment. Current efforts are made, both at national and  
17 international levels to help developing safer MNMs in the market. In order to assess hazards  
18 of MNMs, it is important to take into account exposome parameters in order to link fate and  
19 behavior of MNMs to their potential toxicity. In that context, the aim of this study was to  
20 compare exposure and impact of TiO<sub>2</sub> MNMs-based cement at different levels of its life cycle  
21 (TiO<sub>2</sub>MNMs, cement containing TiO<sub>2</sub> MNMs) between two exposure mesocosm scenarios  
22 mimicking : marine conditions using the bivalve *Scrobicularia plana* and freshwater  
23 conditions using the gastropod *Planorbarius corneus*, for 28 days. These approaches allows  
24 measurements of physical-chemical parameters throughout the duration of the exposure.  
25 Similar results were observed in both exposure conditions since in the two scenarios Ti was  
26 removed from the water column and accumulated in surficial sediments. While in *P. corneus*,  
27 statistically different concentrations of Ti were measured in the digestive glands compared to  
28 controls following exposure to TiO<sub>2</sub> MNMs, elevated background of Ti concentrations were  
29 measured in the controls of *S. plana* that did not allow to discriminating any bioaccumulation  
30 process. In addition, both TiO<sub>2</sub> MNMs and TiO<sub>2</sub>MNM-based cement exposed *S. plana* did not  
31 present any activation of the p38 mitogen-activated protein kinase (MAPKs). This study  
32 demonstrates the challenge of using freshwater-marine continuum using a mesocosm  
33 approach in nanosafety.

34 **Keywords:** Mesocosm, TiO<sub>2</sub>MNMs, *Scrobicularia plana*, *Planorbarius corneus*

## 35 INTRODUCTION

36 Releases of Manufactured Nanomaterial (MNMs) can occur during any stage of the  
37 MNM life cycle i.e. production stage of nanoproduct, the use/application stage of these  
38 nanoproducts and their ultimate end-of-life management/disposal. A comprehensive  
39 understanding of the potential for such releases along the whole life cycle and their possible  
40 effects is crucial to ensure the safe and sustainable use of these new materials (Salieri et al.,  
41 2018). Among all MNMs, TiO<sub>2</sub> MNMs are introduced into many products such as paints,  
42 plastics, food additives, sunscreens and other care products (Yin 2012). The use of TiO<sub>2</sub>  
43 MNMs into cement is a recent application in building material industry. Thanks to its  
44 photocatalytic properties, it confers to the building material air decontamination, self-  
45 sterilizing, self-cleaning and anti-fogging abilities (Jimenez et al., 2016). For those reasons,  
46 photocatalytic cement appears to be an appealing market for industry that represents from 0.1  
47 to 1% of the total European production of TiO<sub>2</sub> and hence about 10.2t to 102t of TiO<sub>2</sub> MNMs  
48 released each year (Nanotechproject.org). TiO<sub>2</sub>MNMs incorporated in the cement matrix are  
49 usually non-coated anatase with a mass concentration ranging from 0.3 to 10 wt% (Ruot et al.,  
50 2009). Degradation of TiO<sub>2</sub> MNM-based cement is likely to happen at each stage of the  
51 cement life cycle (production, manufacturing, use disposal and recycling) (Bossa et al., 2017).  
52 The main causes of release of TiO<sub>2</sub>MNMs from photocatalytic coatings is the stripping of the  
53 TiO<sub>2</sub> from the coatings because of the water flow, the dispersion of agglomerate under NaCl  
54 and UV light condition and finally its discharge from loosening caused by mechanical damage  
55 (Olabarietta et al., 2012). A recent study showed that TiO<sub>2</sub> MNMs were released ( $18.7 \pm 2.1$   
56 to  $33.5 \pm 5.1$  mg of Ti/m<sup>2</sup> of cement after 168 h) from photocatalytic cement pastes that were  
57 leached at a lab-scale to produce a range of degradation rates, meaning that in the worst-case  
58 scenario of weathering a negligible mass of TiO<sub>2</sub> (0.04w.%) was released from the  
59 photocatalytic cement (Bossa et al., 2017). TiO<sub>2</sub> MNMs release comes from a very thin active  
60 surface layer where both the cement surface chemistry and its pore network morphology  
61 control the TiO<sub>2</sub>MNMs diffusion (Bossa, 2019).

62 Laboratory studies have extensively demonstrated the adverse effects of TiO<sub>2</sub> MNMs  
63 on many aquatic organisms (Ramsden et al., 2009; Binh et al., 2016; Hall et al., 2009; Kulacki  
64 et al., 2012). Nevertheless, those studies have been conducted in simple systems (microcosm)  
65 and they did not reflect the MNMs fate and behavior in the environment due to processes such  
66 as sorption and aggregation of MNMs (Auffan et al., 2014). As a consequence, for a strongly  
67 characterization of risk, the combination of the organism, its environment and MNMs needs  
68 to be taken into account and requires interdisciplinary expertise in physical-chemistry,

69 biology and ecotoxicology (Auffan et al., 2014). In that context, mesocosms represent  
70 relevant experimental systems for investigating the complex issue of exposure that enable to  
71 get quantitative time- and spatial data on the distribution of MNMs within a simulated  
72 ecosystem. A mesocosm refers to “an experimental system that simulates real-life conditions  
73 as closely as possible, while allowing the manipulation of environmental factors” (FAO,  
74 2009). As stated during the H2020 European commission funded NANoREG project (Project  
75 #646221), mesocosms have been shown to provide a reliable methodology to obtain  
76 quantitative time- and spatially regarding exposure-driven environmental risk assessment.  
77 In this context, two indoor mesocosm platforms (one marine and one freshwater) were  
78 conceived with small size tanks (60 L) for investigating MNM exposure and impacts on  
79 aquatic species that allows to recreate freshwater and estuarine conditions (sediment, tide  
80 cycles, controlled temperature, salinity and redox potential) (Auffan et al. 2019). TiO<sub>2</sub> MNMs  
81 and TiO<sub>2</sub> MNM-based cement fate, behavior, bioaccumulation and toxicity were evaluated  
82 after a 28 day exposure in two mollusks representative of the estuarine and freshwater  
83 ecosystems : the bivalve *Scrobicularia plana* and the gastropod *Planorbarius corneus*.  
84 *Scrobicularia plana* is an endobenthic bivalve involved in the functioning and the structure of  
85 estuarine ecosystems and has also been largely demonstrated to represent a relevant model for  
86 biomonitoring (Mouneyrac et al., 2014). *Planorbarius corneus* is a hermaphroditic snail that  
87 inhabits small temporary ponds. This species belongs to the *Planorbidae*, the largest family of  
88 aquatic pulmonate gastropods distributed all over the world (Jopp, 2006). *Planorbarius*  
89 *corneus* play an important role in trophic chains as grazer and as prey (Wojdak and Trexler,  
90 2010) and have already been used as model organisms for exposure and toxicity studies in  
91 mesocosms (Tella et al 2014, 2015, Auffan 2018).

92 The originality of the project was to compare the fate and behavior of a nano-enabled product  
93 (TiO<sub>2</sub> MNM-based cement) in these two freshwater and marine ecosystems. Two stages of the  
94 MNM lifecycle were considered : the formulation stage using bare TiO<sub>2</sub>MNMs and end of life  
95 stage of the cement containing TiO<sub>2</sub>MNMs using cement leachate. Freshwater and marine  
96 mesocosms were used to obtain resolved data on the distribution, transformation and impact  
97 towards these mimicked ecosystems depending on the physical-chemical properties of the  
98 environment (salinity, pH, conductivity, tide cycle or not...) and the physical-chemical  
99 properties of the contaminant at two stages of the lifecycle. One of the major drawbacks in  
100 assessing environmental impact of MNMs is that the environmental concentrations are not yet  
101 known. Herein, we used between 1 and 1.2 mg.L<sup>-1</sup> of TiO<sub>2</sub> MNMs which belong to the  
102 threshold values estimated in highly exposed areas (Bourgeault et al., 2015).

## 103 MATERIAL AND METHODS

### 104 *TiO<sub>2</sub>NPs*

105 Primary size and shape of TiO<sub>2</sub> MNMs (NM212, JRC repository) were determined by an  
106 ultra-high resolution scanning electron microscopy SEM LEO 1530 (LEO Electron  
107 Microscopy Ltd, Cambridge, England) and Transmission Electron Microscopy (analytical  
108 TEM Field Emission Gun (FEG) 200 KV Osiris from Tecnai, FEI, Japan). The SEM and  
109 TEM images corroborate the nanometric size of the particles (see SI, figure S1). X-ray  
110 diffraction (XRD) patterns of the samples were obtained using a Bruker D8 X-ray diffraction  
111 (XRD) system in a  $\theta$ -2 $\theta$  mode and Cu K $\alpha$  X-ray source. The TiO<sub>2</sub> MNMs have a body-  
112 centered tetragonal anatase crystal structure (see SI). The width of the XRD peaks were used  
113 to calculate a crystallite size about 9 nm. A specific surface area of 223 m<sup>2</sup>/g was determined  
114 by the Brunauer-Emmett-Teller (BET) adsorption method using the N<sub>2</sub> adsorption isotherm  
115 measured at 77K (BELSORP-max, BEL Japan Inc.).

116

### 117 *TiO<sub>2</sub>MNMs-based cement*

118 Photocatalytic white Portland cement incorporating TiO<sub>2</sub> MNMs was provided by a European  
119 cement manufacturer (Calcia, France) through the French Technical Association of Industries  
120 of Hydraulic Binders (ATILH, France). This cement is mainly composed of Ca and Si ( $\approx$ 66wt  
121 % CaO and  $\approx$ 23 wt% SiO<sub>2</sub>) and contains 2.85 wt% of TiO<sub>2</sub> (anatase) (Bossa et al., 2017).  
122 Cylinders of hardened cement (4 cm diameter, 8 cm high) were obtained after 28 days of  
123 hydration at 20°C with a water/cement ratio of 0.5. Hardened cement pastes exhibit a complex  
124 mineralogy, i.e. a mixture of hydrated minerals (portlandite, calcium silicate hydrates,  
125 ettringite) and residual anhydrous minerals (di and tricalcium silicates). TiO<sub>2</sub>MNMs are  
126 homogeneously dispersed in the hydrated paste, with the exception of few high spots of 50  $\mu$ m  
127 (Bossa et al., 2017).

128 Cement degradation residue generation was simulated using accelerated lab-scale approach to  
129 conduct a so-called « worst-case scenario » and to generate a quantity of cement degradation  
130 residues for mesocosms dosing. Finely crushed cement pastes were leached in batch using  
131 ultra-pure water (UPW) with an elevated liquid-to-solid ratio (L/S) of 100. After pH  
132 stabilization (pH > 12.5), the suspension of cement degradation residues was neutralized with  
133 slow addition of nitric acid (22.37 mol.L<sup>-1</sup>) reach a pH of 7.8 and a conductivity of 13 mS.cm<sup>-1</sup>  
134 <sup>1</sup>. The solution is composed of a dissolved fraction (mainly Ca and Si, 203 and 3.96 mg.L<sup>-1</sup>  
135 respectively) and a particulate fraction with a TiO<sub>2</sub> concentration of 143.7 $\pm$ 2.6 mg.L<sup>-1</sup>. In

136 accordance with the very low TiO<sub>2</sub> MNM solubility, no TiO<sub>2</sub> MNM dissolution was observed  
137 (Table S1). The concentrations of Ca and Si in the dissolved fraction reveal the high  
138 degradability of the cement matrix in natural media (pH 7.8). Presence of free TiO<sub>2</sub> MNMs,  
139 i.e. not embedded in cement matrix, in the solution of cement degradation residues is then  
140 suspected. In neutralized cement degradation residues, TiO<sub>2</sub> MNMs were observed mainly  
141 associated with aggregates larger than 0.45 μm and with SiAl intermix chains. SiAl chains are  
142 supposed to be geopolymers stable at pH 7 and resulting from secondary precipitation/  
143 polymerization during the pH neutralization process (Bossa et al., 2017).

144

### 145 ***Animals***

146 Individuals of *Scrobicularia plana* (15-20 mm length) were hand-collected in November 2015  
147 in the intertidal mudflat on the French Atlantic coast (Bay of Bourgneuf: N 47°01'50.35", W  
148 1°59'04'80") and transported in cool boxes to the laboratory. Then, bivalves were  
149 immediately placed into aerated artificial water (Tropic marin<sup>®</sup>) at 30 practical salinity units  
150 (psu) during 5 days in a temperature controlled room at 15°C (temperature experienced in the  
151 field at the collection time). A natural inoculum containing picoplankton as primary producer  
152 (bacteria, algae, protozoa, etc.) was also collected in the intertidal mudflat. Physico-chemical  
153 parameters of seawater from the collection site were : pH= 7.7; salinity 28 psu; conductivity  
154 40 mS.cm<sup>-1</sup>.

155 Individuals of *Planorbarius corneus* (L., 1758) (Great Ram's Horn snail, benthic grazer)  
156 were hand-collected in October 2015 in a non-contaminated temporary pond part of the  
157 Natura 2000 reserve network in south of France (Bonne Cournes: N 43°20'47.04", E  
158 6°15'34.786", 246 m a.s.l.) and transported in pond water to the laboratory. A natural  
159 inoculum containing picobenthos as primary producer (bacteria, algae, protozoa, etc.) was also  
160 sampled in the pond. Physico-chemical parameters of the pond water from the collection site  
161 were: water temperature 14.9°C; conductivity 819 mS.cm<sup>-1</sup>; concentration of dissolved  
162 oxygen 0.72 mg.L<sup>-1</sup> (6.6%).

163

### 164 ***Mesocosm setup***

165 ***Freshwater mesocosms.*** The mesocosm experiments were already described by Auffan et al.  
166 (2014), Tella et al. (2014), Tella et al. (2015), Auffan et al. (2018)(figure 1). Tanks (750 x 200  
167 x 600 mm) were filled with 6-8 cm artificial sediments containing 89% SiO<sub>2</sub>, 10% kaolinite  
168 and 1% of CaCO<sub>3</sub> w/w adapted from OECD guideline (OECD, 2004). Primary producers  
169 were brought by ~300 g of water-saturated natural sediment (sieved at 200 μm) laid at the

170 surface. The mesocosms were then gently filled with 50 L of Volvic water with pH and  
171 conductivity close to the natural pond water (pH 7, 11.5 mg.L<sup>-1</sup> Ca<sup>2+</sup>, 13.5 mg.L<sup>-1</sup> Cl<sup>-</sup>, 71  
172 mg.L<sup>-1</sup> HCO<sub>3</sub><sup>2-</sup>, 8 mg.L<sup>-1</sup> Mg<sup>2+</sup>, 6.3 mg.L<sup>-1</sup> NO<sub>3</sub><sup>-</sup>, 6.2 mg.L<sup>-1</sup> K<sup>+</sup>, 11.6 mg.L<sup>-1</sup> Na<sup>+</sup>).

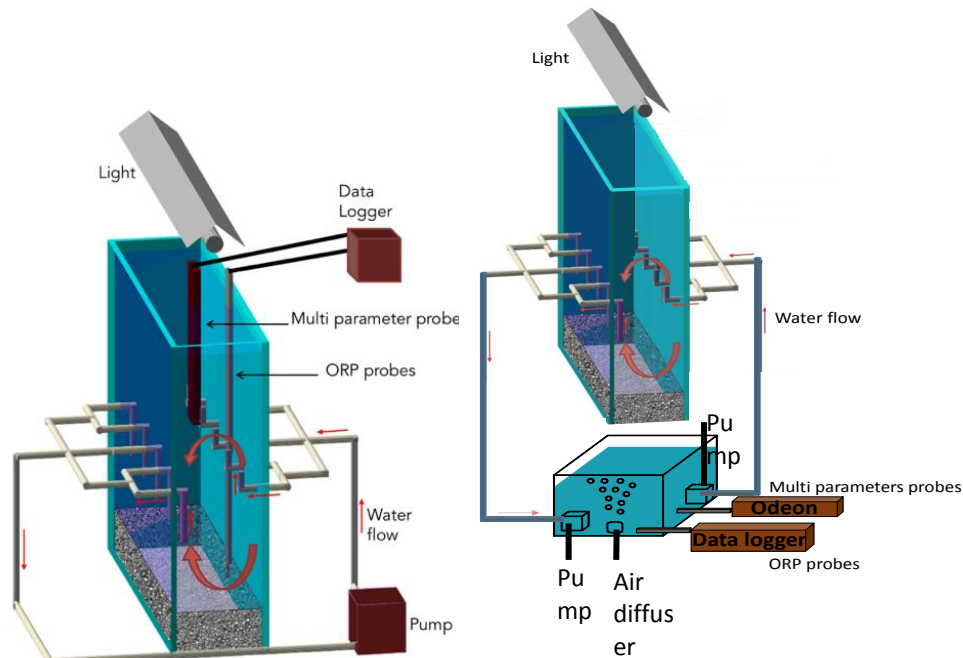
173 After 2 days, the physical-chemical parameters of the mesocosms were stabilized (turbidity,  
174 pH, dissolved O<sub>2</sub>, redox). Then, 19 adult *P. corneus* were added per mesocosm and  
175 acclimatized for one week. Organisms were exposed for 28 days in a temperature controlled  
176 room (18°C) and under controlled light (photoperiod day/night 10:14). Physico-chemical  
177 parameters including temperature (°C), pH, redox potential in the water column and the  
178 sediment (mV), and dissolved oxygen (mg O<sub>2</sub>.L<sup>-1</sup>) were monitored every 2 min during the  
179 whole duration of the experiment. Among the 6 freshwater mesocosms, 2 were kept as  
180 negative control (without contamination), 2 were exposed to TiO<sub>2</sub> MNMs (considered as  
181 positive control), and 2 were exposed to cement leachate. While the first control (negative  
182 control) condition allows to follow animal behavior (mortality) during the experiment, the  
183 second one serve as a positive control experiment to follow TiO<sub>2</sub> bioaccumulation by the  
184 organisms in order to compare with animals treated with cement for both freshwater and  
185 marine systems.

186 .

187 **Marine mesocosms.** Each experimental unit was composed with two tanks (mesocosm and  
188 reserve tank), two pumps (Eheim compact 300L.h<sup>-1</sup>) and a mechanical timer (IDK PMTF  
189 16A) allowing to mimicking the tidal cycle (figure 1). The mesocosm tank (750 x 200 x 600  
190 mm) was filled with 14 kg synthetic sediment (90% SiO<sub>2</sub>, 9% kaolinite, 1% CaCO<sub>3</sub> w/w)  
191 adapted from OECD guideline (OECD, 2004). Three hundred g of water-saturated natural  
192 inoculums was laid at the surface to bring primary producers. Then, each mesocosm tank was  
193 flooded with 35 L of the artificial seawater Tropic Marin™ (Tropicarium Buchshlag Dreieich,  
194 Germany) at 30psu. The reserve tank (700 x 500 x 37 mm) was placed under the first one  
195 (mesocosm tank) to collect removed water from the mesocosm tank during low tide.  
196 Reservoir tank was always filled with a minimum of 25 L of artificial seawater at 30 psu to  
197 constantly maintain the measuring probe immersed.

198 After one week, the physical-chemical parameters of the mesocosms were stabilized  
199 (turbidity, pH, dissolved O<sub>2</sub>, redox). Then, 55 *S. plana* were added per mesocosm and  
200 acclimatized for 5 days. Organisms were exposed for 28 days in a temperature controlled  
201 room (15°C), under controlled light (photoperiod 16:8) and at a tidal cycle (6h of low tide, 6h  
202 of high tide; two tides /day). Physical-chemical parameters including temperature (°C),  
203 salinity (psu), pH, redox potential (mV), dissolved oxygen (mg O<sub>2</sub>.L<sup>-1</sup>) were monitored every

204 15 min into the water column from the reserve tank during the whole duration of the  
205 experiment. Among the 9 marine mesocosms, 3 were kept as negative control (without  
206 contamination), 3 were exposed to TiO<sub>2</sub> MNMs (positive control) and 3 were exposed to  
207 cement leachate.



208

209

**Figure 1.** Scheme of the freshwater (left) and marine (right) mesocosms.

210

### 211 *Mesocosm dosing*

212 Aqueous suspensions of TiO<sub>2</sub> MNMs and TiO<sub>2</sub> MNM-based cement degradation residues  
213 (with a stabilized pH of 7.8) were prepared prior injections in the mesocosms. Aliquots of  
214 these suspensions were digested using an Ultra WAVE microwave digestion system with 1  
215 mL HNO<sub>3</sub> 67% (NORMATOM) and 1 mL HF 47%-51% (PlasmaPure) and analysed by ICP-  
216 MS (Perkin Elmer<sup>®</sup> Nexion 300 ICP-MS) for their total Ti contents. A concentration of  
217  $4.86 \pm 0.13 \text{ g.L}^{-1} \text{ TiO}_2$  (n=3) was found for the TiO<sub>2</sub> MNM suspension ( $2.91 \pm 0.08 \text{ g.L}^{-1} \text{ Ti}$ ). The  
218 TiO<sub>2</sub> concentration measured in the solutions of cement degradation residues (n=6) was  
219  $143.7 \pm 2.6 \text{ mg.L}^{-1}$  ( $86 \pm 1.6 \text{ mg.L}^{-1} \text{ Ti}$ ). Both suspensions were close to the targeted  
220 concentrations and showed excellent recovery yields after digestion (> 95%).

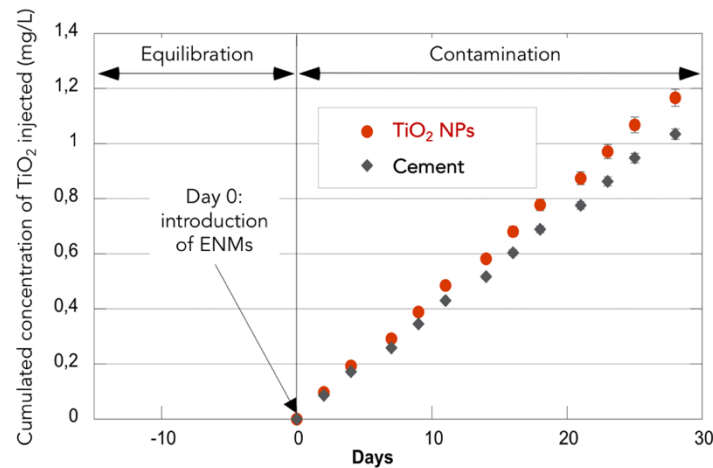
221 A multiple dosing experiment was performed on a 4 week-period. A total of 12 dosings were  
222 achieved (3 times per week), corresponding to  $0.09 \text{ mg.L}^{-1}$  of TiO<sub>2</sub> per injection in order to  
223 reach a final nominal concentration of  $1 \text{ mg.L}^{-1} \text{ TiO}_2$  per mesocosm. As the suspension of  
224 cement degradation residues is not stable over time, a new neutralized batch was prepared  
225 every two injections and stored at 4°C in dark between the two injections.



226 The real concentration injected over time was determined by ICP-MS and are plotted in  
227 Figure 2. For each injection, a low and realistic concentration of  $0.1 \text{ mg.L}^{-1}$  of injected  $\text{TiO}_2$   
228 was targeted in the mesocosm ( $0.06 \text{ mg.L}^{-1}\text{Ti}$ ). After 30 days (12 injections), the cumulated  
229 concentration of  $\text{TiO}_2$  injected reached  $1\text{-}1.2 \text{ mg.L}^{-1}$  in the mesocosms.

230

231



232

233 **Figure 2.**  $\text{TiO}_2$  injection sequence for  $\text{TiO}_2$ MNMs and  $\text{TiO}_2$ MNM-based cement degradation  
234 residues in both freshwater and marine mesocosms over the 28 days-contamination period.

235

### 236 *Ti quantification in the different compartment of the mesocosms*

237 The concentration of Ti in the mesocosms following  $\text{TiO}_2$  MNMs or cement leachate  
238 contamination was measured in the water column, in the surficial sediments and in the  
239 organisms sampled at 0, 7, 14, 21 and 28 days. Water was sampled at ~10cm from the  
240 air/water interface. Surficial sediments (between 500  $\mu\text{m}$  to 1000  $\mu\text{m}$  depth) were sampled at  
241 three different locations and then pooled before being dried. Samples were digested using  
242 microwaves at  $180^\circ\text{C}$  before analysis by ICP-MS.

243 For the marine mesocosms, Ti quantifications were performed by Micropolluants Technologie  
244 S.A. (Metz, France) using an Agilent 7700 ICP-MS (Agilent Technologies France). 10 mL of  
245 water or 2 mL of surficial sediments were mixed with 1mL 32-35% HCl, 1mL 67-69%  $\text{HNO}_3$ ,  
246 100  $\mu\text{L}$  94-98%  $\text{H}_2\text{SO}_4$ , and 1 mL 47-51% HF prior ICP-MS measurements. For *S. plana*,  
247 whole soft tissues were mixed with 1 mL 67-69%  $\text{HNO}_3$ , 100  $\mu\text{L}$  94-98%  $\text{H}_2\text{SO}_4$ , and 1 mL  
248 47-51% HF. For the freshwater mesocosms, water samples (2 mL) were digested with 1 mL  
249  $\text{HNO}_3$  67-69% and 0.5 mL HF 47%-51%. For the surficial sediments (50 mg), a mixture of 3  
250 acids (1 mL HCl 34%, 2 mL  $\text{HNO}_3$  67%, 0.5 mL HF 47%-51%) was used. For *P. corneus*, the

251 digestive glands were dissected, before being digested using 1 mL HNO<sub>3</sub> 67%, 0.5 mL H<sub>2</sub>O<sub>2</sub>  
252 30%-32% and 1 mL HF 47%-51%. Samples were digested using the microwave Ultra WAVE  
253 and the analysis were performed using the Perkin Elmer Nexion 300 ICP-MS. Using  
254 sediments and freshwater organisms spiked with TiO<sub>2</sub> nanoparticles, a recovery yield of  
255 >95% after microwave digestion and ICP-MS analysis was obtained.

256

### 257 ***Evaluation of immunotoxic effects in S. plana: pp38 level measurement by Western blot***

258 Total whole soft tissues of *S. plana* exposed for 28 days (n=7 for each condition) were  
259 homogenized with lysis-buffer (NaCl 0.2M, DTT 1mM, protease inhibitor cocktail 0.1%) in a  
260 mortar at 4°C. The clear supernatant was then obtained by centrifugation (13,000xg, 10 min,  
261 4°C) and stored at -20°C until analysis. Protein concentrations were determined according to  
262 Bradford (1976) using bovine serum albumin as a standard. Protein extracts were mixed with  
263 sample buffer (0.5 M Tris-HCl, pH 6.8, 2% SDS, 10% glycerol, 4% 2-mercaptoethanol,  
264 0.05% bromophenol blue) 1:3 and boiled for 5 min at 95°C. Proteins (40 µg per lane) were  
265 separated using a 12% polyacrylamide gel. Western blot analysis was performed as previously  
266 described (Châtel et al., 2011b). After transfer, membranes were incubated with a mouse  
267 monoclonal antibody anti-Phospho-p38 MAPK (Thr<sub>180</sub>/Tyr<sub>182</sub>) (9216-Cell signaling  
268 Biotechnology) diluted in 1/1000 in TBS/BSA 5% or with a mouse monoclonal antibody anti-  
269 β-Actin (A5441 -SIGMA) diluted in 1/2000 in TBS/BSA 5%. After washing (3 times for 5  
270 min), membranes were incubated with a goat anti-Mouse IgG antibody coupled with alkaline  
271 phosphatase (A3562, Sigma Aldrich) diluted 1:2000 in TBS/BSA 5%. Detection of immune  
272 complexes was carried out by colorimetric reaction using a solution of 5-bromo-4-chloro-3-  
273 indolyl phosphatase (BCIP) and nitroblue tetrazolium (NBT). After visualization, membranes  
274 were scanned and band intensity, which is the relative amount of protein expression, was  
275 quantified as Relative Optical Densities (ROD; pixels/mm<sup>2</sup>). Results of pp38 were normalized  
276 according to actin expression.

277

### 278 ***Statistical analysis***

279 The measured values were compared among different groups using the non-parametric test  
280 Mann-Whitney (XL-Stat software) and the Student's t-test. Statistical significance was  
281 accepted at p<0.05.

282

283

284

## 285 **RESULTS and DISCUSSION**

286

### 287 *Favorable physical-chemical conditions in freshwater and estuarine mesocosms*

288 During the 28 days of contamination several physical-chemical parameters were monitored to  
289 assess the global response of the mesocosms to the presence of TiO<sub>2</sub> MNMs and cement  
290 leachate. In marine as well as in freshwater mesocosms, the average temperature, dissolved  
291 O<sub>2</sub>, conductivity, and pH were not significantly different between negative controls and  
292 contaminated mesocosms(see SI, Figures S2 and S3).

293 Oxido-reductive probes indicated that freshwater was oxidative (310±20 mV), while reductive  
294 conditions prevailed in the sediments (ca -370 mV). Regarding the conductivity, a step by  
295 step increase from day 0 to day 28 (200 ± 1 μS.cm<sup>-1</sup> to 288 ± 0.4 μS.cm<sup>-1</sup>respectively) was  
296 observed. Conductivity drops were recorded during the weekly refills with ultrapure water to  
297 compensate the evaporation. On the whole, no significant differences were observed between  
298 controls and contaminated mesocosms.

299 Consequently, during the exposure to TiO<sub>2</sub> MNMs and cement leachate, the physico-chemical  
300 conditions of the 15 mesocosms remained favorable with the oxygenation, pH, temperature,  
301 redox potential in the range of natural conditions.

302

### 303 *Homo-aggregation of TiO<sub>2</sub> MNMs and accumulation in the surficial sediments*

304 Bossa et al. (2017) estimated using an accelerated aging protocol that a negligible mass of  
305 TiO<sub>2</sub> (0.04w.%) was released from the photocatalytic cement (Bossa et al., 2017). Herein, we  
306 used an accelerated lab-scale approach to conduct a so-called « worst-case scenario »  
307 assuming that 100% of the Ti contained in the cement would have been released. Figure 3 and  
308 4 show the Ti concentrations measured in the water column and sediments of both freshwater  
309 and marine mesocosms as a function of time. Ti was detected in both waters and sediments  
310 sampled in control mesocosms proving that a high geochemical background of this element  
311 existed in the mimicked ecosystems. Average background Ti concentrations in freshwater  
312 mesocosms were 19.2±17.2 μg.L<sup>-1</sup> in the water column and 2230±928 mg.kg<sup>-1</sup> in surficial  
313 sediments. Average background Ti concentrations in marine control mesocosms were  
314 567±273mg.kg<sup>-1</sup> in surficial sediments and below the quantification limit (<2.5 μg.L<sup>-1</sup>) in the  
315 water column. Ti is a naturally occurring element in mineral and amorphous phases occurring  
316 in freshwater and marine environments. Ti can be found in titanium-iron oxide minerals (as  
317 ilmenite), TiO<sub>2</sub> minerals as rutile, anatase, and brookite. Herein, the TiO<sub>2</sub> MNMs used were  
318 engineered nanosized anatase minerals. Consequently even if the Ti background concentration

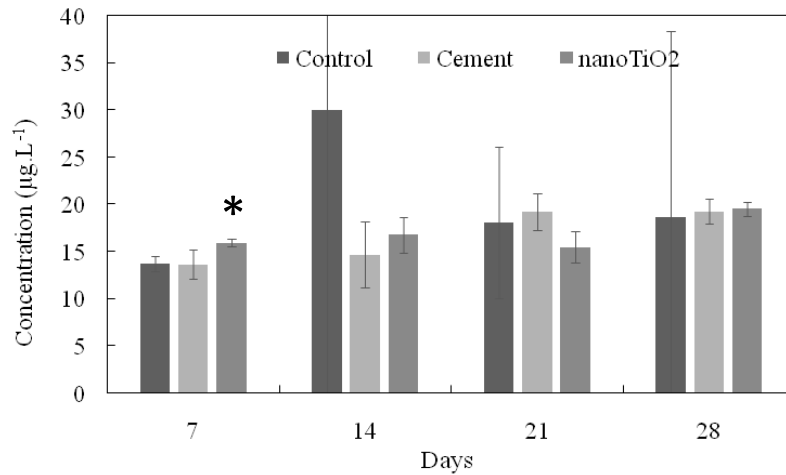
319 was elevated, it is noteworthy that the speciation and reactivity of the naturally occurring Ti-  
320 bearing phases might be different from the MNM injected.

321 In the surficial sediments of marine mesocosms, high concentrations of Ti were detected after  
322 7 days (control, TiO<sub>2</sub> MNMs, and cement leachate) and progressively decreased until 28 days  
323 (Figure 4, right). However, because of the elevated geochemical background of Ti, no  
324 statistical difference was observed between controls and contaminated mesocosms. Similarly,  
325 no increase in Ti concentration could be evidenced in the surficial sediments of contaminated  
326 freshwater mesocosms compared to controls. Besides, the fluctuations of Ti concentration  
327 measured over time were likely related to the heterogeneity of the Ti distribution and the  
328 difficulty of sampling the surficial sediments(Figure 4). These results highlighted the  
329 challenge of a reliable quantification of Ti in that compartment.

330

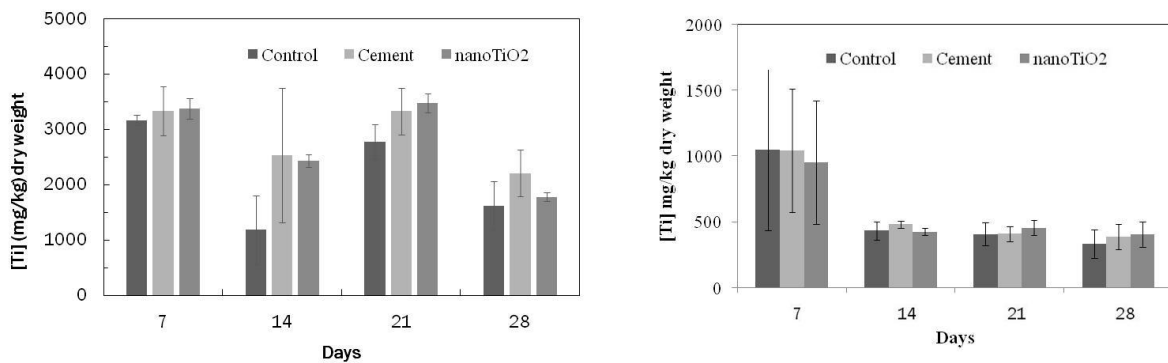
331 Total Ti concentrations in the water column of marine mesocosms (control, TiO<sub>2</sub> MNMs and  
332 cement leachate) were always below the quantification limit estimated at 2.5 µg.L<sup>-1</sup> whatever  
333 the duration of exposure. On the opposite, total Ti concentrations in the water column were  
334 always above 10 µg.L<sup>-1</sup> in freshwater mesocosms. The only condition for which a statistically  
335 significant difference was observed between the water column of controls and contaminated  
336 freshwater mesocosms was after 7 days of exposure to TiO<sub>2</sub> MNMs. At this time point, the  
337 difference between TiO<sub>2</sub> MNMs contaminated mesocosms and geochemical Ti background  
338 were 2.2±1.2 µg.L<sup>-1</sup>Ti for a total Ti concentration injected of 180 µg.L<sup>-1</sup>Ti (300 µg.L<sup>-1</sup> of  
339 TiO<sub>2</sub>). Based on these values, we estimated that 98-99 % of the Ti injected was removed from  
340 the water column after 7 days. Although no increase in Ti concentration could be evidenced in  
341 the surficial sediment of freshwater mesocosms, we hypothesize that both cement leachate  
342 and TiO<sub>2</sub> MNMs settled at more than 98% at the surface of sediments. Based on the 31.0±0.6  
343 mg and 35.0±0.9 mg Ti introduced respectively after 28 days in mesocosms contaminated  
344 with cement leachate and TiO<sub>2</sub> MNMs, the remaining of 2% of Ti particles in the water  
345 column should entail a theoretical increase in the surficial sediment of 176 mg.kg<sup>-1</sup>, which is  
346 far below the standard deviation determined for Ti background in that compartment. This  
347 explains why Ti accumulation at sediment surface remained undetected by chemical analysis.  
348 In addition, in marine mesocosms, due to the tidal system, part of the sediment were removed  
349 along with the water in the lower tank and sedimentation of TiO<sub>2</sub> occurred as well in this  
350 compartment favoring decrease in its concentration as compared to freshwater mesocosms.

351



352  
353  
354  
355  
356  
357

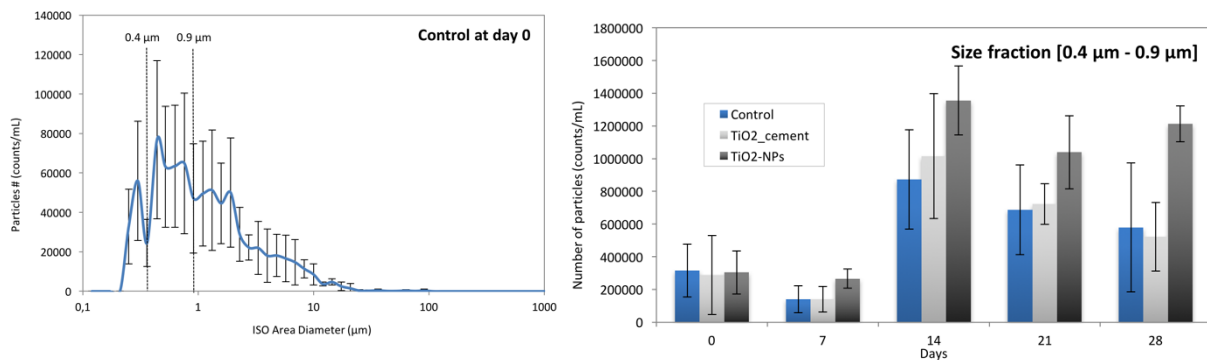
**Figure 3.** Total Ti concentration in the water column after 7, 14, 21 and 28 days of exposure in freshwater mesocosms. Ti concentration in the water column in marine mesocosms is not represented as values were always below the quantification limit estimated at  $2.5 \mu\text{g.L}^{-1}$ . Statistical significance was determined by the Student's t-test (\*:  $p < 0.05$ ).



358  
359  
360  
361  
362  
363  
364  
365  
366  
367  
368  
369  
370  
371  
372

**Figure 4.** Total Ti concentration in surficial sediment after 7, 14, 21 and 28 days of exposure in freshwater (left) and marine (right) mesocosms.

In freshwater mesocosms, the size distribution of the suspended matter in the  $0.1 \mu\text{m} - 1000 \mu\text{m}$  size range and the total number of suspended particles in the  $0.4 \mu\text{m} - 0.9 \mu\text{m}$  size range were not different between control and contaminated mesocosms (Figure 5). This highlighted that the main mechanism of aggregation and settling down expected in the water column was the homo-aggregation of the  $\text{TiO}_2$  MNMs either pristine or brought *via* cement leachate. In marine mesocosms, MNM homo-aggregation was expected to be even faster due to higher alkalinity and ionic strength as compared to freshwater environments (Peralta-Videa et al., 2011; Rocha et al., 2015; Vale et al., 2016). It is noteworthy that the aggregation of MNMs allows their deposition onto the surficial sediment (Peralta-Videa et al., 2011), resulting in high exposure of benthic organisms compared to planktonic organisms (Mohd Omar et al., 2014; Mouneyrac et al., 2014).



373

374 **Figure 5.** (left) Size distribution of colloidal particles in the water column of freshwater  
 375 control mesocosms at day 0. The dotted lines mark out the 0.4 µm – 0.9 µm fraction. (right)  
 376 Evolution of the number of colloidal particles in the 0.4µm – 0.9 µm range from day 0 to 28,  
 377 under the three conditions tested (control, cement leachate and TiO<sub>2</sub> MNMs) in freshwater  
 378 mesocosms.

379

### 380 *Bioaccumulation and effects on benthic organisms*

381 *P. corneus* and *S. plana* are two benthic grazer species. While *P. corneus* eat algae and  
 382 biofilms at the sediment/water interface(Jones 1961), *S. plana* can either feed suspended  
 383 particles from the water column but also ingest sedimentary particles (Hughes, 1969). For *S.*  
 384 *plana* exposed in marine mesocosms, elevated background of Ti concentrations were  
 385 measured in the control group (84.8±42.3 mg.kg<sup>-1</sup> dry weight) which did not allow to  
 386 discriminating any bioaccumulation process in organisms exposed to TiO<sub>2</sub> MNMs and cement  
 387 leachate (97.1±43.9 and 107.5±48.2 mg.kg<sup>-1</sup> dry weight, respectively) (figure 6).

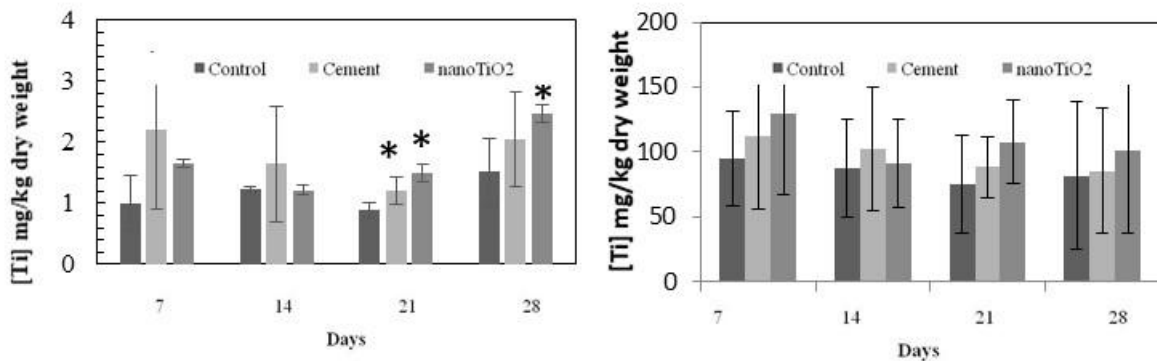
388 Background concentrations of Ti measured in the digestive glands of unexposed *P. corneus*  
 389 were one order of magnitude lower. Following exposure to cement leachate, no difference in  
 390 Ti concentration in the digestive glands were measured with respect to control *P. corneus*.  
 391 However, statistically different concentrations of Ti were measured in the digestive glands  
 392 compared to controls following exposure to TiO<sub>2</sub> MNMs *i.e.* 1.5 ± 0.2 mg Ti.kg<sup>-1</sup> (dry weight)  
 393 and 2.5 ± 0.1 mg Ti.kg<sup>-1</sup> (dry weight) after 21 and 28 days of exposure respectively (figure 6).  
 394 This suggests that an ingestion of Ti by *P. corneus* occurred likely resulting from the  
 395 accumulation of TiO<sub>2</sub> MNMs on the surficial sediments.

396 Some authors have shown abilities to discriminate natural Ti from TiO<sub>2</sub> NMs. For example,  
 397 Bourgeault et al. (2015) resolved this lack of sensitivity using isotopically modified TiO<sub>2</sub>  
 398 nanoparticles (<sup>47</sup>Ti) to characterize the processes governing Ti bioaccumulation in a  
 399 freshwater environment. Thanks to the <sup>47</sup>Ti labeling, they detected bioaccumulation of NPs in  
 400 *Dreissena polymorpha* exposed for 1 h at environmental concentrations *via* water (7–120  
 401 µg/L of <sup>47</sup>TiO<sub>2</sub> NPs) and *via* their food (4–830 µg/L of <sup>47</sup>TiO<sub>2</sub> NPs mixed with 1 × 10<sup>6</sup>

402 cells/mL of cyanobacteria) despite the high natural Ti background, which varied in individual  
403 mussels. Such a methodology would be particularly relevant in mesocosms experiment  
404 mimicking real environments with high Ti background.

405

406



407

408 **Figure 6.** Total Ti concentration in the digestive gland of *P. corneus* (left) and total soft  
409 tissues of *S. plana* (right) after 7, 14, 21 and 28 days of exposure in mesocosms. The  
410 statistical significant was determined by the Student's t-test (\*:  $p < 0.05$ ; \*\*:  $p < 0.01$ ).

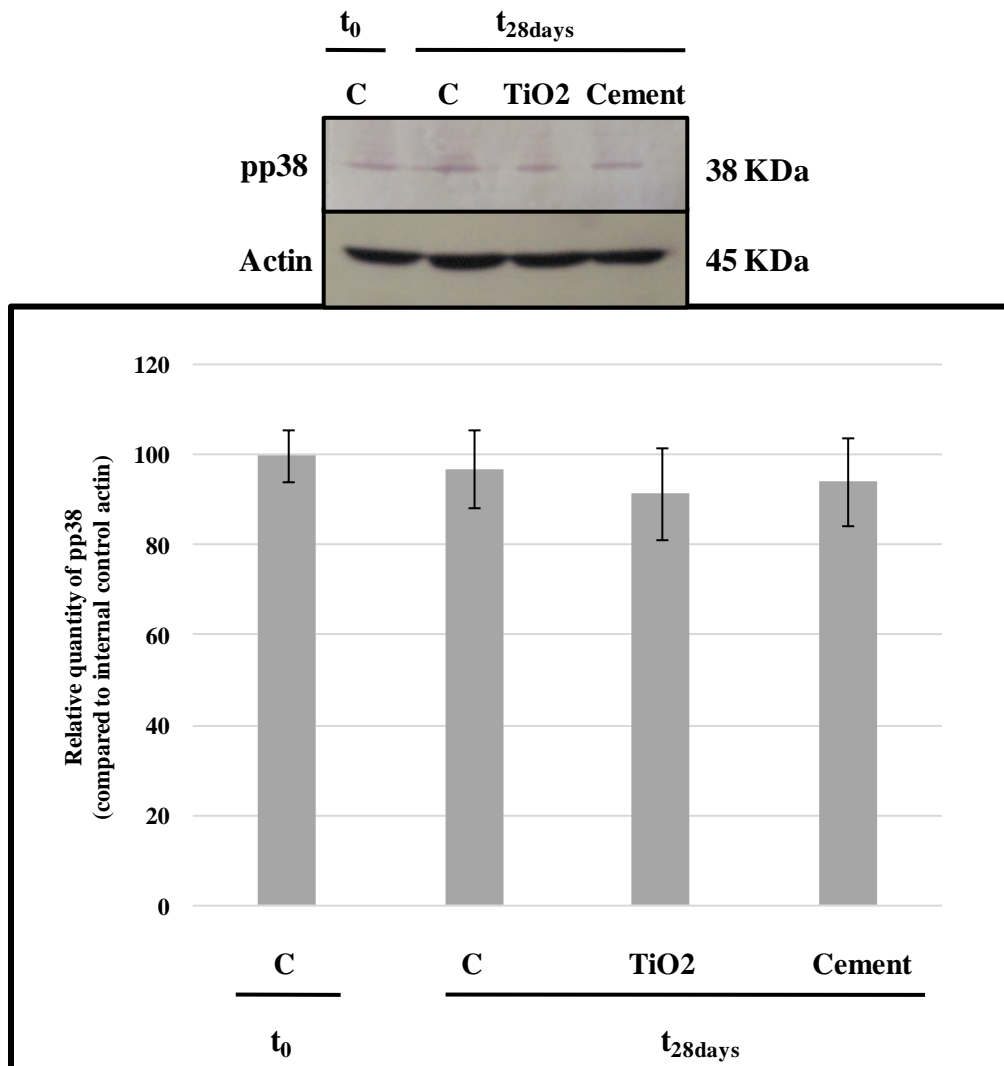
411

412 During the 28 days of exposure in mesocosms, the survival rates of *P. corneus* and *S. plana*  
413 (<2% of mortality, data not shown), picoplankton and picobenthos (see SI, Figure S4) were  
414 not affected by the presence of TiO<sub>2</sub> MNMs and cement leachate. Hence, no acute toxicity  
415 was observed towards these two trophic levels. Nevertheless, a thorough characterization of  
416 the biological responses (at the individual, sub-individual, and community levels) is still  
417 needed to better understand the biological mechanisms of interactions.

418 One of the main effect associated with TiO<sub>2</sub> toxicity was the induction of immune responses.  
419 The MAPKs represent a superfamily of protein Ser/Thr-kinases, highly conserved through  
420 evolution (Kyriakis and Avruch, 2001; Roux and Blenis, 2004), that can transduce stress  
421 signals into cellular responses (Kultz and Avila, 2001; Kyriakis and Avruch, 2001). Three  
422 subfamilies of the MAPKs have been well described in mammals: the extracellular regulated  
423 protein kinase (ERK), the c-Jun NH<sub>2</sub>-terminal kinases (JNK) and the p38-MAPK. ERKs have  
424 been more associated to cell division, growth and differentiation whereas JNKs and p38-  
425 MAPKs are activated in various types of stress going from osmotic stress to chemical stress  
426 and can trigger cell survival or death (apoptosis), depending on their isoform and/or cell type  
427 (Canesi et al., 2001, 2002, 2006; Châtel et al., 2009, 2011a,b). They have been demonstrated  
428 to play a key role in immune responses in mammals (Caffrey et al., 1999) but also in  
429 invertebrates and more particular in bivalves (Canesi et al., 2001; 2002; 2006). Moreover p38



430 MAPK have been shown to be induced by TiO<sub>2</sub> exposure in bivalves (Couleau et al., 2012).  
431 P38 MAPK in *S. plana* have been studied in the laboratory and antibody matching has already  
432 been verified on this specie as opposed to *P. corneus*. Since no ingestion of Ti by *S. plana* was  
433 identified by ICP-MS, western blot analysis of *S. plana* using specific antibodies directed  
434 against the phosphorylated form of p38 MAPK were used (Figure 7).  
435 In the present study, membrane revelation showed that the molecular weight of pp38 in *S.*  
436 *plana* is around 38 KDa. After normalization of the different bands representing pp38  
437 expression with actin, results revealed that there was no significant modification in pp38  
438 expression level for any of the conditions tested (TiO<sub>2</sub> MNMs or cement leachate), as  
439 compared to control group (figure 7). This suggested no stimulation of immune response of *S.*  
440 *plana* following 28 days of exposure. Couleau et al. (2012) observed in the freshwater mussel  
441 *D. polymorpha* exposed to TiO<sub>2</sub> (0.1 to 25 mg.L<sup>-1</sup> during 24 h), that ERK ½ was activated for  
442 all concentrations tested in this study whereas p38 activation was only observed when  
443 bivalves were exposed to 5 and 25 mg.L<sup>-1</sup>) indicating that p38 phosphorylation was less  
444 sensitive than ERK ½ to this contaminant. This could be the case in the present study.  
445 Moreover, an *in vitro* *M. galloprovincialis* hemocyte exposure to TiO<sub>2</sub> (10 µg.ml<sup>-1</sup>) for 5 to 60  
446 min showed that pp38 activation was transient, with an increase in phosphorylated form of  
447 p38 after 5 and 15 min, followed by a dephosphorylation at 30 and 60 min (Canesi et al.,  
448 2010). Even though p38 is implicated in immune responses, absence of p38 activation does  
449 not mean that immune response is not present. However, in the present study, the long  
450 duration of exposure (28 days) could explain the absence of pp38 response depicted in *S.*  
451 *plana* and investigation of its response at shorter time points would have been interesting to  
452 perform.



453

454 **Figure 7.** Expression of pp38 in *S. plana* control, TiO<sub>2</sub> MNMs or cement leachate, analyzed  
 455 by Western blot. Results have been normalized to actin expression levels.

456

457 **Conclusion**

458 In the present study, impact of TiO<sub>2</sub> MNMs and TiO<sub>2</sub> MNM-based cement leachate was  
 459 investigated in marine and freshwater mesocosms, that allows to reproduce realistic  
 460 environmental exposure (mid-term duration, low doses, chronic contamination,...) and in  
 461 particular, a tidal system in the marine mesocosm. Such tools have been demonstrated as  
 462 being relevant since they take into account both hazard and exposure and hence the synergetic  
 463 and/or antagonistic effects of different physico-chemical parameters (temperature, pH, redox  
 464 potential, conductivity), that is of great interest for the regulation of the use of NMs (Auffan  
 465 et al., 2019).The originality of the project was also to compare the exposure and potential  
 466 impact of TiO<sub>2</sub> and cement containing TiO<sub>2</sub> MNMs on two species, representative of the  
 467 estuarine/freshwater continuum(with a salinity gradient),that are particular targets towards

468 nanomaterials at the water/sediment interface. The use of similar design for both freshwater  
469 and marine systems showed challenging points and limitations, that enable consistent  
470 comparison of fate and behavior of NMs in different species. However, even with same  
471 procedures, characterization of TiO<sub>2</sub> in different abiotic compartments was difficult, as stated  
472 in this study, and made challenging investigations of differences in bioaccumulation and  
473 effects in these benthic species. The standardization of stable test suspensions for  
474 nanomaterials is an ongoing challenge as it is well documented that the preparation method  
475 influences the interpretation of toxicity according to the exposure. In the context of  
476 developing a regulatory framework this is a challenge as it necessary that all nanomaterials  
477 have equivalent preparation techniques in order to have a better standardization of  
478 experiments and hence a more comparable set of data generated for nanomaterial-related data  
479 categorization.

480 Finally, studying the impact of TiO<sub>2</sub> at different stages of the TiO<sub>2</sub> MNMs life cycle allows  
481 identifying critical stages at which Safe by design (SbD) concepts can be implemented to  
482 reduce adverse impacts or decrease exposure to MNMs.

483

484

485 **REFERENCES**

486 Auffan, M., Tella, M., Santaella, C., Brousset, L., Paillès, C., Barakat, M., Espinasse, B.,  
487 Artells, E., Issartel, J., Masion, A., Rose, J., Wiesner, M.R., Achouak, W., Thiéry, A. and  
488 Bottero, J.Y., 2014. An adaptable mesocosm platform for performing integrated assessments  
489 of nanomaterial risk in complex environmental systems. *Sci. Rep.* 4, 5608.  
490 <https://doi.org/10.1038/srep05608>

491  
492 Auffan, M., Masion, A., Mouneyrac, C., de Garidel-Thoron, C., Hendren, C., Thiery, A.,  
493 Santaella, C., Giamberini, L., Bottero, J.Y., Wiesner, M. and Rose, J., 2019. Contribution of  
494 mesocosm testing to a single-step and exposure-driven environmental risk assessment of  
495 engineered nanomaterials. *NanoImpact.* 13, 66-69.  
496 <https://doi.org/10.1016/j.impact.2018.12.005>

497  
498 Auffan, M., Liu, W., Brousset, L., Scifo, L., Pariat, A., Sanles, M., Chaurand, P., Angeletti,  
499 B., Thiery, A., Masion, A. and Rose, J., 2018. Environmental Exposure of a Simulated Pond  
500 Ecosystem to Cuo Nanoparticle Based-Wood Stain Throughout Its Life Cycle. *Environ. Sc.:*  
501 *Nano.* 5, 2579-2589. <https://doi.org/10.1039/C8EN00712H>

502  
503 Bour, A., Mouchet, F., Cadarsi, S., Silvestre, J., Verneuil, L., Baqué, D., Chauvet, E.,  
504 Bonzom, J. M., Pagnout, C., Clivot, H., Fourquaux, I., Tella, M., Auffan, M., Gauthier, L.  
505 and Pinelli, E., 2016. Nanoparticles on a freshwater experimental trophic chain: A study in  
506 environmentally relevant conditions through the use of mesocosms. *Nanotoxicology.* 10 (2),  
507 245-55. <https://doi.org/10.3109/17435390.2015.1053422>

508  
509 Bourgeault, A., Cousin, C., Geertsen, V., Cassier-Chauvat, Chauvat, C., F., Duruphy, O.,  
510 Chanéac, C. and Spalla, O., 2015. The challenge of studying TiO<sub>2</sub> nanoparticle  
511 bioaccumulation at environmental concentrations: crucial use of a stable isotope tracer.  
512 *Environ. Sci. Technol.* 49(4), 2451-9. <https://doi.org/10.1021/es504638f>

513  
514 Caffrey, D.R., O'Neill, L.A.J. and Shields, D.C., 1999. The evolution of the MAP kinase  
515 pathways: coduplication of interacting proteins leads to new signaling cascades. *J. Mol. Evol.*  
516 49, 576- 582. <http://dx.doi.org/10.1007/PL00006578>

517 Canesi, L., Betti, B., Ciacci, M. and Gallo, G., 2001. Insulin-like effect of zinc in *Mytilus*  
518 digestive gland cells: modulation of tyrosine kinase-mediated cell signaling. *Gen. Comp.*  
519 *Endocrinol.* 122, 60-66. <https://doi.org/10.1006/gcen.2001.7612>

520 Canesi, L., Betti, M., Ciacci, C., Scarpato, A., Citterio, B., Pruzzo, C. and Gallo, G., 2002.  
521 Signaling pathways involved in the physiological response of mussel hemocytes to bacterial  
522 challenge: the role of stress-activated p38 MAP kinases. *Dev. Comp. Immunol.* 26, 325-334.  
523 [https://doi.org/10.1016/S0145-305X\(01\)00078-7](https://doi.org/10.1016/S0145-305X(01)00078-7)

524 Canesi, L., Ciacci, C., Lorusso, L.C., Betti, M., Guarnieri, T., Tavolari, S. and Gallo, G.,  
525 2006. Immunomodulation by 17 beta-estradiol in bivalve hemocytes. *Am. J. Physiol. Regul.*  
526 *Integr. Comp. Physiol.* 291, R664-673. <https://doi.org/10.1152/ajpregu.00139.2006>

527 Canesi, L., Ciacci, C., Vallotto, D., Gallo, G., Marcomini, A. and Pojana, G., 2010. *In vitro*  
528 effects of suspensions of selected nanoparticles (C60 fullerene, TiO<sub>2</sub>, SiO<sub>2</sub>) on *Mytilus*  
529 hemocytes. *Aquat. Toxicol.* 96 (2), 151-8. <https://doi.org/10.1016/j.aquatox.2009.10.017>

530 Châtel, A., Hamer, B., Talarmin, H., Dorange, G., Schroder, H.C. and Muller, W.E., 2009.  
531 Activation of MAP kinase signaling pathway in the mussel *Mytilus galloprovincialis* as  
532 biomarker of environmental pollution. *Aquat. Toxicol.* 96, 247-255.  
533 <https://doi.org/10.1016/j.aquatox.2009.11.002>

534 Châtel, A., Talarmin, H., Hamer, B., Schroder, H.C., Muller, W.E. and Dorange, G., 2011a.  
535 MAP kinase cell signaling pathway as biomarker of environmental pollution in the sponge  
536 *Suberites domuncula*. *Ecotoxicology.* 20, 1727-1740. [http://dx.doi.org/10.1007/s10646-011-](http://dx.doi.org/10.1007/s10646-011-0706-1)  
537 [0706-1](http://dx.doi.org/10.1007/s10646-011-0706-1)

538 Châtel, A., Hamer, B., Jaksic, Z., Vucelic, V., Talarmin, H., Dorange, G., Schroder, H.C. and  
539 Muller, W.E. 2011b. Induction of apoptosis in mussel *Mytilus galloprovincialis* gills by  
540 model cytotoxic agents. *Ecotoxicology.* 20, 2030-2041. [https://doi.org/10.1007/s10646-011-](https://doi.org/10.1007/s10646-011-0746-6)  
541 [0746-6](https://doi.org/10.1007/s10646-011-0746-6)

542 Couleau, N., Techer, D., Pagnout, C., Jomini, S., Foucaud, L., Laval-Gilly, P., Falla, J.  
543 and Bennisroune, A., 2012. Hemocyte responses of *Dreissena polymorpha* following a short-  
544 term in vivo exposure to titanium dioxide nanoparticles: preliminary investigations. *Sci. Total*  
545 *Environ.* 438, 490-7. <https://doi.org/10.1016/j.scitotenv.2012.08.095>

546 Farré, M., Gajda-Schranz, K., Kantiani, L. and Barceló, D., 2009. Ecotoxicity and analysis of  
547 nanomaterials in the aquatic environment. *Anal. Bioanal. Chem.* 393,81-95.  
548 <https://doi.org/10.1007/s00216-008-2458-1>  
549

550 Hughes, R.N., 1969. A study of feeding in *Scrobicularia plana*. *J. mar. biol. Ass. U.K.* 49,  
551 805-823. <https://doi.org/10.1017/S0025315400037309>  
552

553 Jones, J. D., 1961. Aspects of Respiration in *Planorbis Corneus* L. And *Lymnaea Stagnalis* L.  
554 (Gastropoda: Pulmonata). *Comp. Biochem. Physiol.* 4,1-29. [https://doi.org/10.1016/0010-](https://doi.org/10.1016/0010-406X(61)90042-1)  
555 [406X\(61\)90042-1](https://doi.org/10.1016/0010-406X(61)90042-1)  
556

557 Kyriakis, J.M. and Avruch, J., 2001. Mammalian mitogen-activated protein kinase signal  
558 transduction pathways activated by stress and inflammation. *Physiol. Rev.* 81, 807-869.  
559 <https://doi.org/10.1152/physrev.2001.81.2.807>  
560

561 Kultz, D. and Avila, K., 2001. Mitogen-activated protein kinases are *in vivo* transducers of  
562 osmosensory signals in fish gill cells. *Comp. Biochem. Physiol. B. Biochem. Mol. Biol.*  
563 129,821-829. [https://doi.org/10.1016/S1096-4959\(01\)00395-5](https://doi.org/10.1016/S1096-4959(01)00395-5)  
564

565 Mohd Omar, F., Abdul Aziz, H. and Stoll, S., 2014. Aggregation and disaggregation of ZnO  
566 nanoparticles: Influence of pH and adsorption of Suwannee River humic acid. *Sci. Total*  
567 *Environ.* 468–469,195–201. <https://doi.org/10.1016/j.scitotenv.2013.08.044>  
568

569 Mouneyrac, C., Linot, S., Amiard, J.C., Amiard-Triquet, C., Métais, I., Durou, C., Minier, C.  
570 and Pellerin, J., 2008. Biological indices, energy reserves, steroid hormones and sexual  
571 maturity in the infaunal bivalve *Scrobicularia plana* from three sites differing by their level of  
572 contamination. *Gen. Comp. Endocrinol.* 157(2), 133-141.  
573 <https://doi.org/10.1016/j.ygcen.2008.04.010>  
574

575 Peralta-Videa, J.R., Zhao, L., Lopez-Moreno, M.L., de la Rosa, G., Hong, J. and Gardea-  
576 Torresdey, J.L., 2011. Nanomaterials and the environment: a review for the biennium  
577 2008–2010. *J. Hazard. Mater.* 186, 1-15. <https://doi.org/10.1016/j.jhazmat.2010.11.020>  
578

579 Rocha, M., Fernandes, C., Pereira, C., Rebelo, S.L.H., Pereira, M.F.R. and Freire, C., 2015.  
580 Gold-supported magnetically recyclable nanocatalysts: a sustainable solution for the reduction  
581 of 4-nitrophenol in water. *RSC Adv.* 5, 5131-5141. <https://doi.org/10.1039/c4ra15865b>  
582

583 Roux, P.P. and Blenis, J., 2004. ERK and p38 MAPK-activated protein kinases: a family of  
584 protein kinases with diverse biological functions. *Microbiol. Mol. Biol. Rev.* 68, 320-344.  
585 <https://doi.org/10.1128/MMBR.68.2.320-344.2004>  
586

587 Tella, M., Auffan, M., Brousset, L., Issartel, J., Kieffer, I., Pailles, C., Morel, E., Santaella, C.,  
588 Angeletti, B., Artells, E., Rose, J., Thiery, A., Bottero, J.Y., 2014. Transfer, Transformation  
589 and Impacts of Ceria Nanomaterials in Aquatic Mesocosms Simulating a Pond Ecosystem.  
590 *Environmental Science & Technology.* 48, 9004–9013. <https://doi.org/10.1021/es501641b>  
591

592 Tella, M., Auffan, M., Brousset, L., Morel, E., Proux, O., Chaneac, C., Angeletti, B., Pailles,  
593 C., Artells, E., Santaella, C., Rose, J., Thiery, A., Bottero, J.Y., 2015. Chronic Dosing of a  
594 Simulated Pond Ecosystem in Indoor Aquatic Mesocosms: Fate and Transport of CeO<sub>2</sub>  
595 Nanoparticles. *Environmental Science-Nano.* 2, 653-663.  
596 <http://dx.doi.org/10.1039/C5EN00092K>  
597

598 Vale, G., Mehennaoui, K., Cambier, S., Libralato, G., Jomini, S. and Domingos, R.F., 2016.  
599 Manufactured nanoparticles in the aquatic environment-biochemical responses on freshwater  
600 organisms: A critical overview. *Aquat. Toxicol.* 170,162-174.  
601 <https://doi.org/10.1016/j.aquatox.2015.11.019>  
602  
603  
604  
605  
606  
607

608 **ACKNOWLEDGEMENTS**

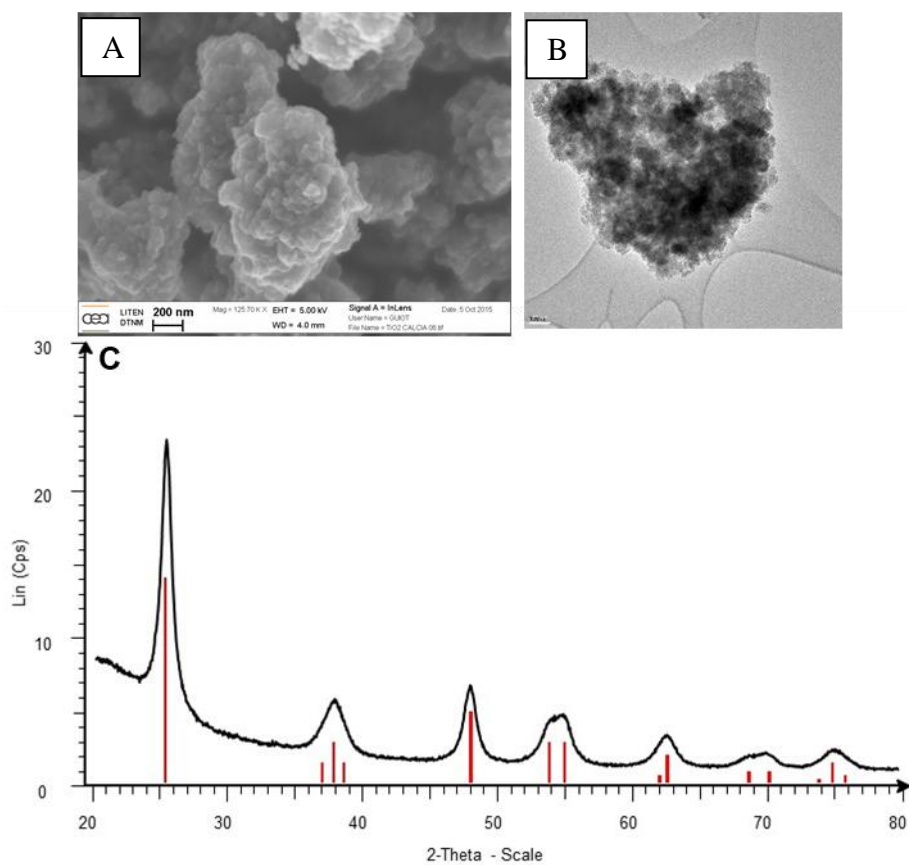
609 The research leading to these results has received funding from the European Research  
610 Council under the European Union's FP7 Grant Agreement n.310584 (NANoREG project).  
611 The authors wish to thank L. Izoret (ATILH, Paris, France) for providing cements, as well as  
612 A. Guiot, S. Artous, S. Jacquinot and O. Sicardy (CEA, Grenoble, France) for their  
613 participation to the characterization of the raw materials. The TEM used in this study was part  
614 of Nano-ID platform which was funded by the EQUIPEX project ANR-10-EQPX-39-01. Part  
615 of this study was also funded via the French ANR through the ANR-3-CESA-0014/  
616 NANOSALT program, and the Excellence Initiative of Aix- Marseille University -  
617 A\*MIDEX, a French “Investissementsd'Avenir” program through its associated Labex  
618 SERENADE project. This work was also a contribution to the OSU-InstitutPythéas. Finally,  
619 the authors acknowledge the CNRS funding for the international research project IRP iNOVE.

620

621

622





624  
625 **Figure S1.** Primary size and shape of TiO<sub>2</sub>MNMs determined by an ultra-high resolution  
626 scanning electron microscopy (SEM) (A) and Transmission Electron Microscopy (TEM) (B).  
627 Body-centered tetragonal anatase crystal structure of TiO<sub>2</sub>MNM observed by X-ray  
628 diffraction (XRD) (C).  
629

630 **Table 1.** Concentrations of Ti, Ca, Al, Fe, Ca and Si after cement degradation in the total  
631 (dissolved + particulate fractions) and soluble fraction solution  
632

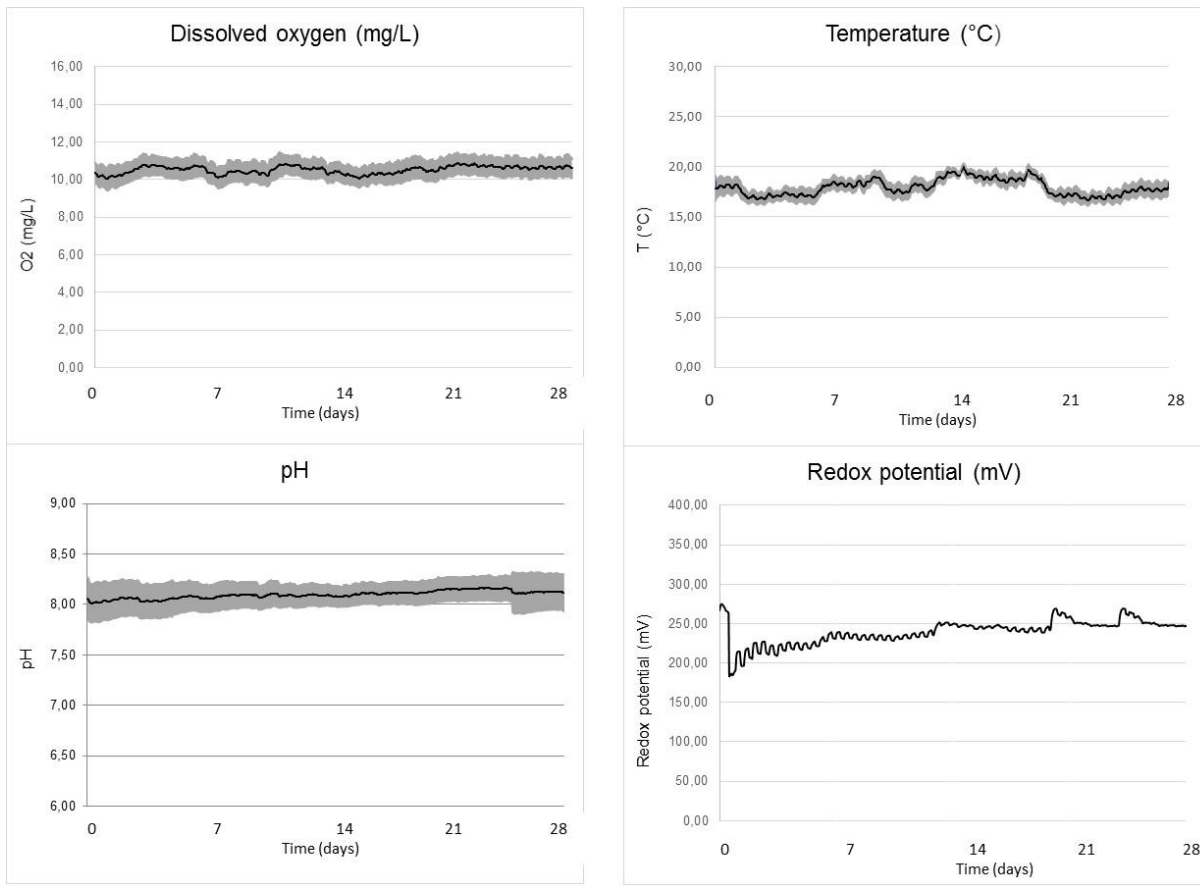
	Ti	Na	Al	Fe	Ca	Si
Total (mg.L <sup>-1</sup> )	<b>89.91</b>	1.89	54.06	12.10	2216.00	2407.80
Soluble fraction (<3 kDa) (µg/l)	3.22	182.00	1.00	1.00	2.03E+05	3960.00

633

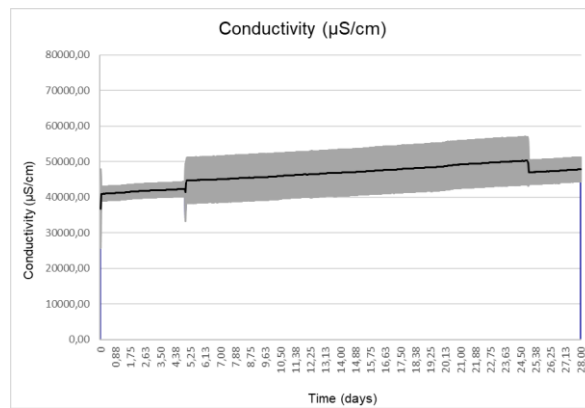
634

635

636



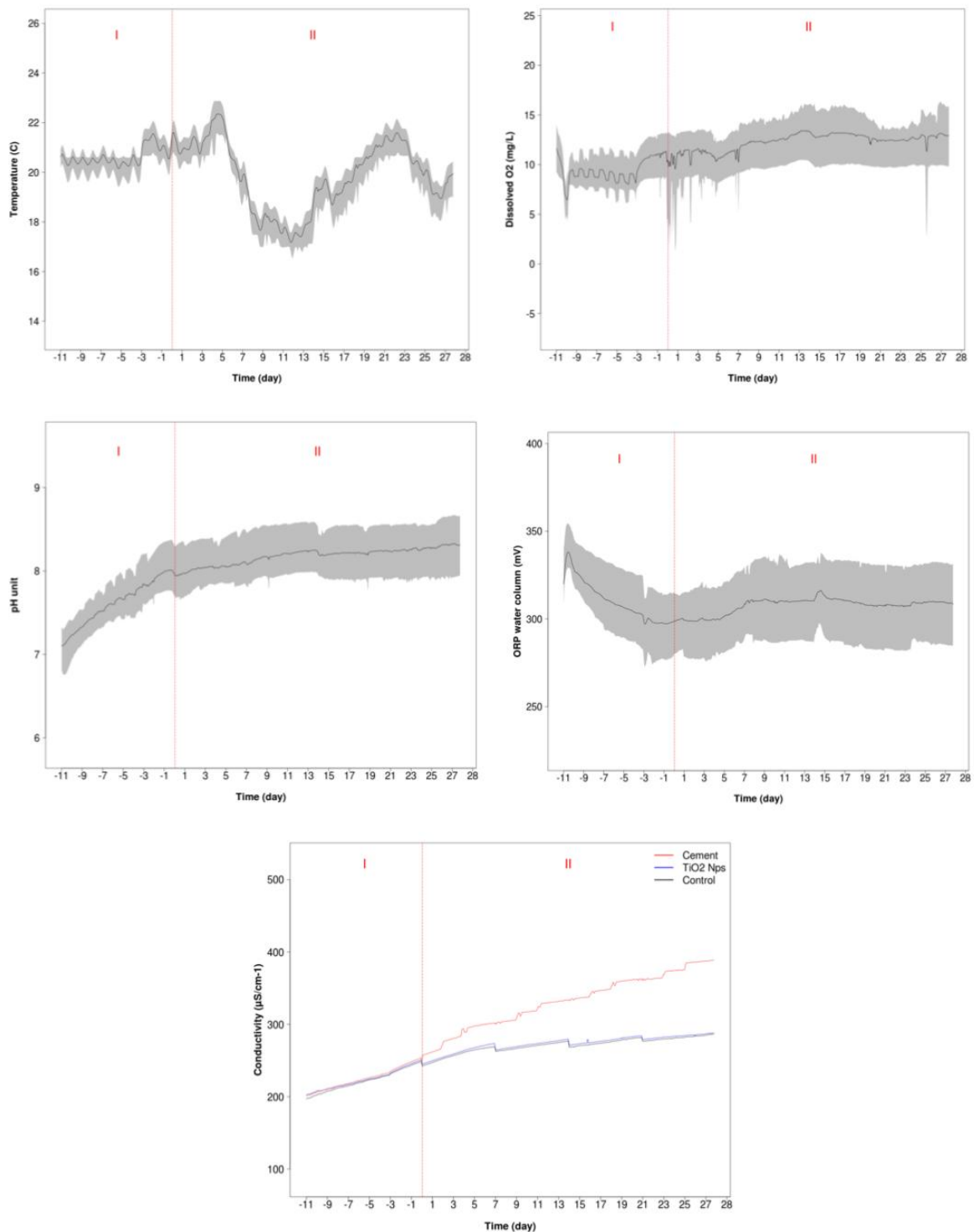
637



638

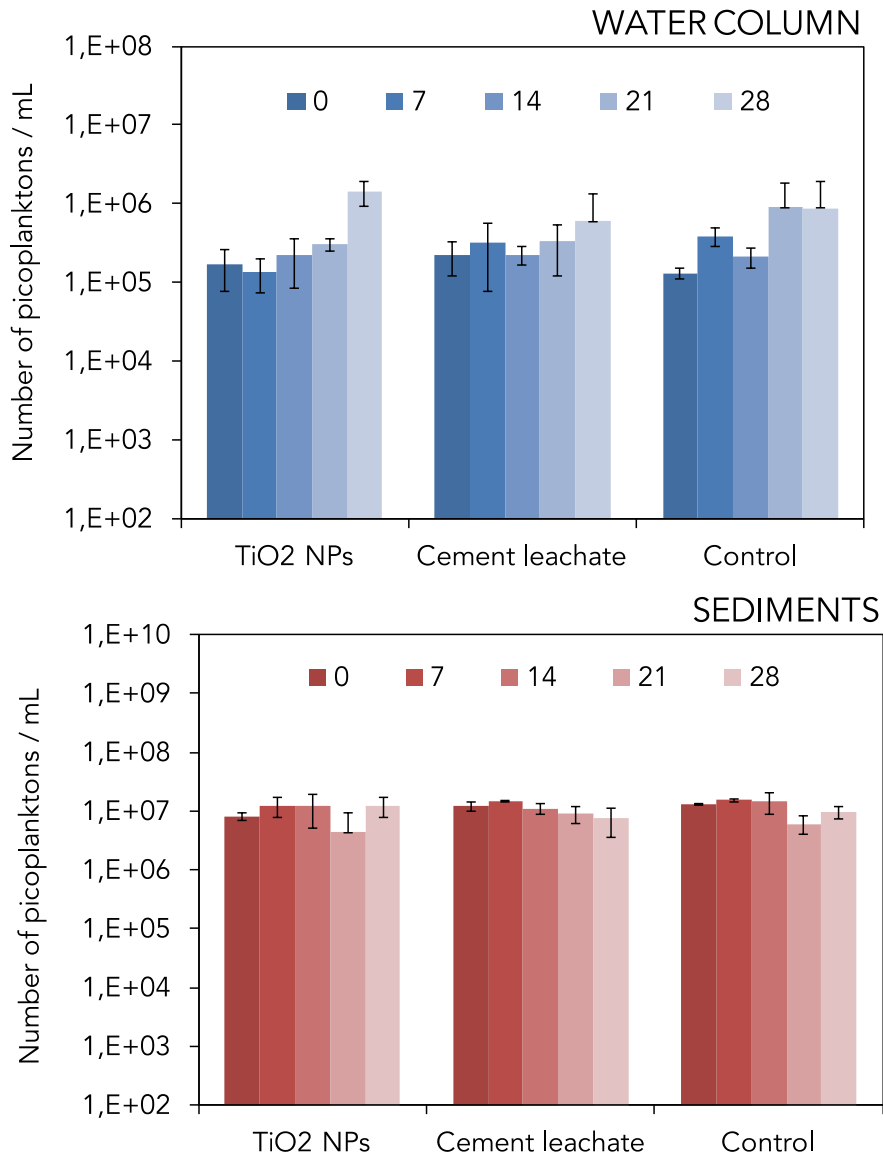
639 **Figure S2.** Evolution of the physical-chemical parameters in the water column of the marine  
640 mesocosms. Temperature, Redox potential, dissolved oxygen, pH were measured during  
641 phases I (stabilization) and II (contamination). Day 0 corresponds to the first dosing of NPs.  
642 The grey surface is defined by the maximum and minimum values of each parameter, and the  
643 dark line corresponds to the average values of the 9 mesocosms. One measurement was  
644 performed every 5 min.

645



647

648 **Figure S3.** Evolution of the physical-chemical parameters in the water column of the  
 649 freshwater mesocosms. Oxidation-Reduction potential (ORP), dissolved oxygen, pH, and  
 650 conductivity were measured during phases I (stabilization) and II (contamination). Day 0  
 651 corresponds to the first dosing of NPs. The grey surface is defined by the maximum and  
 652 minimum values of each parameter, and the dark line corresponds to the average values of the  
 653 6 mesocosms. The conductivity were not merged since a different trend was observed in the  
 654 mesocosms exposed to cement leachate. One measurement was performed every 5 min.



655

656

657 **Figure S4.** Concentration of picoplankton in water column at 10 cm below water surface  
 658 (Top) and in surficial sediments(depth: 0.5 to 1 mm) (B)on a weekly basis.

659 Five mL of water and 15 mL of sediment were sampled, treated with formaldehyde (3.7%),  
 660 and stored at 4°C before counting. Before picoplankton counting, 1 mL of each water column  
 661 sample was centrifuged ( $5.9 \times g$  at 4°C for 15 min), and 200  $\mu\text{L}$  of each sediment sample was  
 662 treated with 800  $\mu\text{L}$  of 0.1 mM sterile tetrasodium pyrophosphate and vortexed with a steel  
 663 ball for 30 seconds. For the counting, 10  $\mu\text{L}$  of each sample was mixed with 5 $\mu\text{L}$  of 3 $\mu\text{M}$   
 664 SYTO® 9 Green Fluorescent Nucleic Acid Stain and dropped on a glass slide. Concentration  
 665 of picoplankton was the mean  $\pm$  standard deviation of five counts.

666

667

668